10

Rotary Kiln Minerals Process Applications

The processes that employ the rotary kiln as the primary reactor are many and they encompass all industries including food, dedicated dryers, minerals processing, and so on. We will focus on minerals and materials processing and provide some of the key industrial processes that use a rotary kiln as the primary workhorse. As we saw from the history of cement in Chapter 1, rotary kiln technology as we know it today evolved from the struggles of the early engineers and inventors to produce cement and lime in an efficient, safe, and economic way. It is only prudent that we begin this chapter with these processes. We will first describe the cement and lime processes, then move on to describe some of the carbothermic reduction processes that employ the rotary kiln as the primary device. Here we will examine two processes, iron ore reduction (the SLRN process) and illmenite ore reduction (the Becher process). We will then examine the lightweight aggregate process.

10.1 Lime Making

Lime manufacturing is one of the oldest processes known to man, having been carried out since prehistoric times. The remains of fossils, according to geologists, formed the limestone bed thousands of

years ago. The abundance of limestone as well as high magnesium limestone, called dolomite, in much of the world, have played an important part in the development of many area communities. Limestone is a rock composed of calcium, carbon, and oxygen. When it is heated, the carbon escapes as carbon dioxide, leaving calcium oxide, which is known as quicklime or, simply, lime. This process is what is called lime burning or limestone "calcinations." In the United States, probably the first settlement to obtain lime from limestone was in Rhode Island, followed by the Quakers when they settled in Philadelphia and Dutch settlers of the Hudson River valley (Oats, 1998). It has been reported that cargoes of lime were shipped by boat from Maine to Boston and New York City in the early 1800s. The lime burning industry we see today came into prominence at the end of the 1890s. With so much suitable stone readily available and right at hand, it was natural that the first homes should have used lime burnt on the site. Hence, there were several lime kilns operating in many areas of the United States at the time. Surface stones were cracked for burning in kilns that were originally fired by wood. Often large kilns were set in cliff faces as the sea winds assisted the burning process. However, much of the work was manual, including the crushing, until the crusher machine was designed which was used primarily to crush limestone for road beds.

Lime was and still is used in soil stabilization, road building, chemical manufacture, the tanning process, and the purification of water, whitewashing buildings, treating animal hides and leather, and for plaster and mortar. The US National Lime Association tends to think that lime is "the versatile chemical."

10.2 Limestone Dissociation (Calcination)

When limestone (calcium carbonate) is heated, it dissociates into quicklime and carbon dioxide in a process known as calcination. The calcination reaction follows.

$$\mathrm{CaCO_3(s)} \Leftrightarrow \mathrm{CaO(s)} + \mathrm{CO_2(g)} \tag{10.1}$$

where s and g denote solid and gaseous states. The equilibrium Gibbs free energy of the reaction at atmospheric pressure ($p_o = 1$), can be expressed as a function of temperature, that is,

$$\Delta G^{o}_{rx} = 182837 + 13.402T \ln T - 251.059T \quad [\mathrm{Jmol^{-1}}] \tag{10.2}$$

Recall that,

$$\Delta G^{\circ}_{\mathrm{rx}} = -RT \ln K_e$$
$$\ln K_e = -\frac{21990}{T} - 1.6119 \ln T + 30.196 \tag{10.3}$$

We assume that the activities of the solid phases are equal to unity. For the gaseous phase, the activity is a function of the dissociation pressure; therefore the partial pressure of CO_2 at equilibrium with $CaCO_3$ is (Themelis, 1995)

$$P_{\mathrm{CO}_{2,e}} \approx K_e p_{\mathrm{o}} \tag{10.4}$$

HSC calculations show that decomposition will proceed at about 900°C. An alternative means of attaining decomposition at a lower temperature than 900°C is to decrease the bulk concentration of CO_2 in the reactor by providing a flow of air, or any other gas with the exception of CO_2, over the decomposing limestone. The task is to select the appropriate reactor with the least heat transfer resistance so as the reactor temperature is well above the dissociation temperature necessary to accomplish the reaction. We will examine the appropriate heat transfer resistances later. The heat of reaction can be estimated from Table 10.1.

$$\mathrm{CaCO_3} = \mathrm{CaO} + \mathrm{CO_2} \qquad \Delta \mathrm{H} = -1768\,\mathrm{kJ/kg}(-760\ \mathrm{Btu/lb})\ \mathrm{CaCO_3} \tag{10.5}$$

Magnesium carbonate, which is found in some quantities with limestone deposits, also dissociates as according to the reaction

$$\mathrm{MgCO_3} = \mathrm{MgO} + \mathrm{CO_2} \qquad \Delta \mathrm{H} = -1298\,\mathrm{kJ/kg}(-558\ \mathrm{Btu/lb})\ \mathrm{MgCO_3} \tag{10.6}$$

For the purpose of feedstock quality classification, mineral deposits that contain a significant amount of $MgCO_3$ (5–39 percent) are called dolomitic limestone, while those containing >40 percent are known as dolomite.

The dissociation of both calcium and magnesium carbonate is endothermic and needs elevated temperature to drive the reaction (see Figures 10.1 and 10.2). The reaction rate increases with increasing temperature. For magnesium carbonate, the reaction commences at 250°C (480°F) and requires 410°C (770°F) to go to completion at atmospheric pressure (Figure 10.2) compared with calcium carbonate

Table 10.1 HSC Calculations

$CaCO_3 = CaO + CO_2(g)$					
T (°C)	**ΔH (kcal)**	**ΔS (cal/K)**	**ΔG (kcal)**	**K**	**log(K)**
0	42.604	38.345	32.13	1.95×10^{-26}	−25.709
100	42.475	37.954	28.313	2.61×10^{-17}	−16.584
200	42.258	37.442	24.543	4.60×10^{-12}	−11.337
300	41.99	36.928	20.824	1.15×10^{-08}	−7.941
400	41.68	36.432	17.156	2.69×10^{-06}	−5.571
500	41.334	35.952	13.537	1.49×10^{-04}	−3.827
600	40.949	35.485	9.965	3.20×10^{-03}	−2.495
700	40.525	35.026	6.44	3.58×10^{-02}	−1.446
800	40.062	34.573	2.96	2.50×10^{-01}	−0.603
900	39.556	34.123	−0.475	1.23	0.088
1,000	39.007	33.674	−3.864	4.61	0.663
1,100	38.416	33.227	−7.209	1.41×10^{1}	1.148
1,200	37.781	32.78	−10.51	3.63×10^{1}	1.559

Formula	**MW (g/mol)**	**Concentration (wt-%)**	**Amount (mol)**	**Amount (g)**	**Volume**
$CaCO_3$	100.089	100	1	100.089	36.933 mL
CaO	56.079	56.029	1	56.079	16.79 mL
$CO_2(g)$	44.01	43.971	1	44.01	22.414 L

where the reaction occurs between 500–805°C (930–1480°F). However, the decomposition of dolomites and magnesium/dolomitic limestone precursors is more complex than for their pure compounds. It is still not clear whether the decomposition reactions proceed in a single path, two discrete paths, or a combination of both (Oats, 1998), that is,

$$CaCO_3 \cdot MgCO_3 + \text{Heat} = CaCO_3 \cdot MgO + CO_2 \tag{10.7}$$

$$CaCO_3 \cdot MgO + \text{Heat} = CaO \cdot MgO + CO_2 \tag{10.8}$$

$$CaCO_3 \cdot MgCO_3 + \text{Heat} = CaO \cdot MgO + CO_2 \tag{10.9}$$

All dolomites and magnesium/dolomite limestone decompose at higher temperatures than magnesium carbonate with the onset of

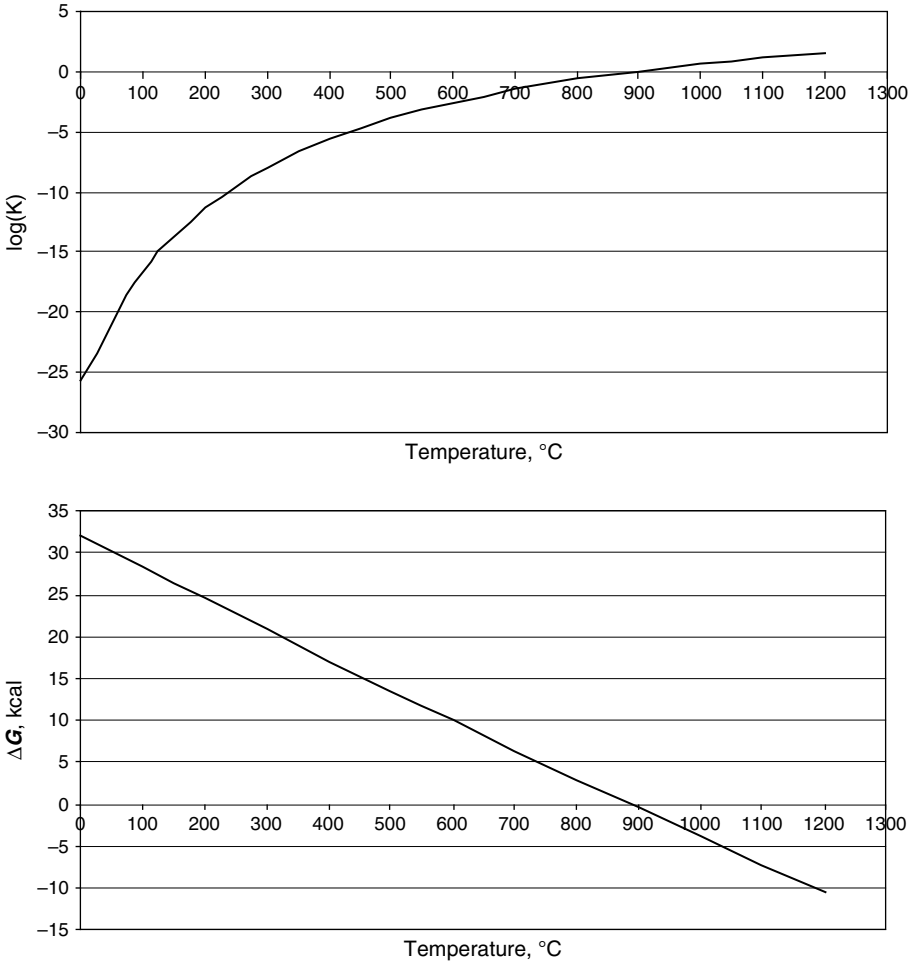

Figure 10.1 Equilibrium decomposition of calcium carbonate as a function of temperature.

the dissociation varying between 510 and 750°C. If the feedstock is heated to temperatures much greater than 900°C, the quicklime product can become very dense with very low internal surface area and is described as overburnt. Overburning results in low reactivity lime, which, although useful for certain applications such as refractory linings, is unacceptable for many chemical applications. The temperature at which overburning becomes serious is about 1400°C for pure limestone, and may be as low as 1200°C for some of the less pure materials.

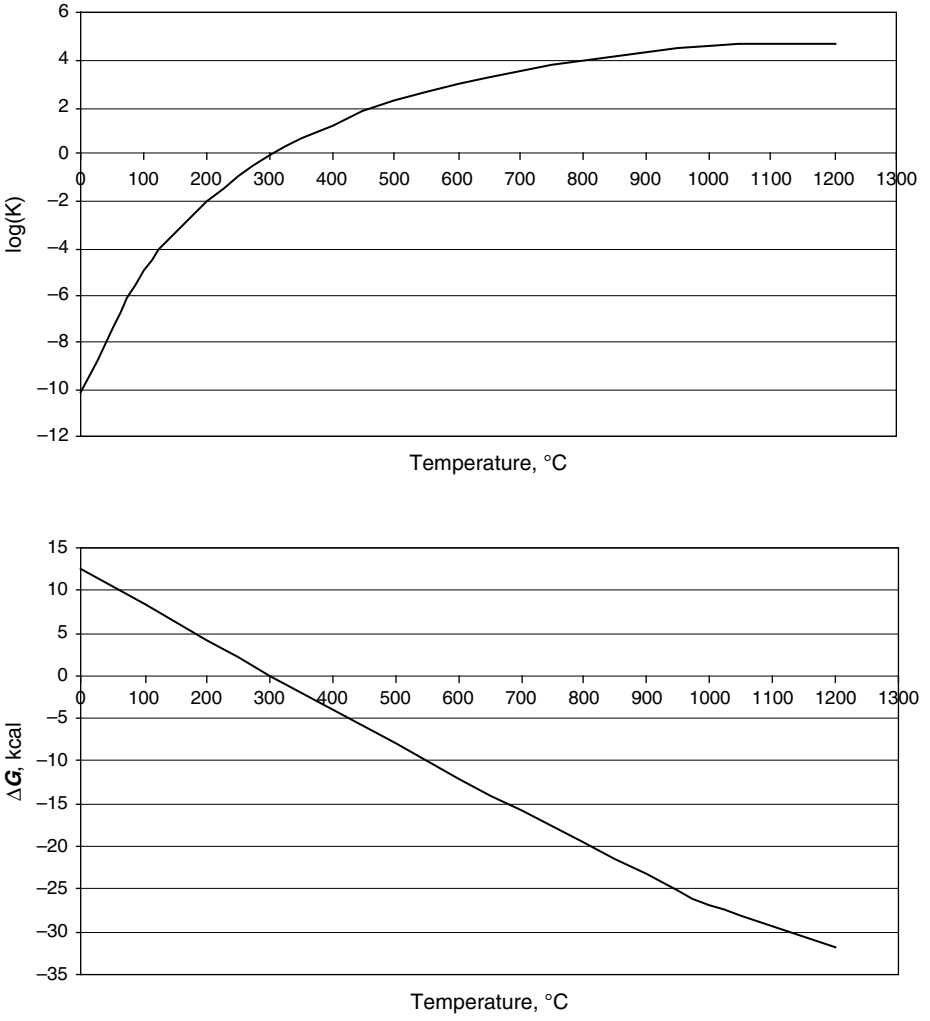

Figure 10.2 Equilibrium decomposition of magnesium carbonate as a function of temperature.

For the many applications of quicklime, active lime is the preferred product, hence careful control of the dissociation (calcination) process is necessary, bearing in mind that the time required for complete calcination depends on factors such as kiln temperature, stone size, and porosity of feed material. The dissociation of limestone above the decomposition temperature is a heterogeneous reaction (Figure 10.3).

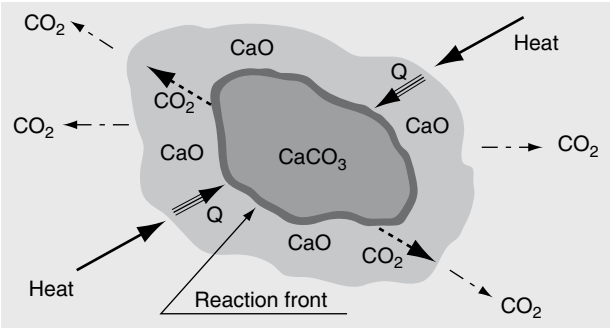

Figure 10.3 Limestone dissociation process steps.

This dissociation can be regarded as being made up of the five process steps.

1. Heat is transferred from the furnace gases to the surface of the decomposing particle.
2. This is followed by heat conduction from the surface to the reaction front through the micro-porous lattice structure of lime.
3. Heat arrives at the reaction front and causes the dissociation of $CaCO_3$ into CaO and CO_2.
4. The CO_2 produced migrates from the reaction front, through the lime layer, to the particle surface.
5. CO_2 migrates away from the particle surface into the kiln's atmosphere.

Each of these events poses some degree of resistance to the overall process of achieving complete dissociation (calcination) and can be an impediment to achieving quality product. The step controlling the process will ultimately be the one with the highest degree of resistance. Since the decomposition reaction is fast once the particle attains the appropriate temperature, perhaps the rate controlling step will depend upon how fast one can get the heat to the reaction front and get rid of the CO_2 accumulated at the front so as to prevent recarbonation of the quicklime already formed. Hence, process development and the evolution of lime kiln design over the years have been based on mixing

that improves heat and mass diffusion. The selection of the appropriate kiln technology, the kiln's dimensions, and internal mixing aid structures such as lifters, as well as operational procedures such as feed particle size distribution, are all factors that influence effective heat transfer to the material and the gas diffusion to the atmosphere.

10.3 The Rotary Lime Kiln

From the fuel requirement point of view, rotary kilns are the most flexible of all lime kilns (Oates, 1998). They are successfully fired with natural gas, fuel oil, and pulverized fuels of all types including coal, coke, and sawdust. According to Boynton (1980) the United States is by far the world's leader in rotary kiln lime production with about 88 percent of its commercial and about 70 percent of captive plant capacity provided by kilns. The conventional rotary lime kiln has a length-to-diameter (L/D) ratio in the 30–40 range with lengths of 75–500 ft (22.7–152.5 m) and diameter of 4–11 ft (1.2–3.3 m). Lime kilns are usually inclined at about a 3–5° slope with material charged at the elevated end and discharging at the lower end. The degree of fill is relatively deep, about 10–12 percent. Owing to its low thermal conductivity limestone with a large diameter of about 2 in. (5 cm) results in higher effective bed heat conduction than smaller stones. The larger feed material sizes tend to have larger pore volume in the bulk and thereby maximizes the particle-to-particle heat transfer which is usually dominated by radiation at the dissociation temperatures. The smaller feed stones tend to pack themselves upon rotation and render the bed a poor conductor of heat. For many years most long kilns operated with deplorable fuel efficiencies because of poor or lack of heat recuperation such as coolers and preheaters (Figure 10.4) with thermal consumption as high as 12–15 million Btu/ton (3336–4170 kcal/kg) of lime. Thanks to ingenious heat recuperation systems such as coolers, preheaters, lifters, and so on, today thermal efficiencies of rotary lime kilns are in the 6–8 million Btu/ton range (1668–2224 kcal/kg), using fuel at about half the rate of early long kilns.

Some rotary lime kilns operate under reducing conditions by curtailing the combustion air to substoichiometric levels so as to volatilize any sulfur that may be in the limestone in order to meet the stringent sulfur specifications imposed by steel and chemical users. For most operations except for dead-burnt dolomite, the burner tip velocities

Figure 10.4 Photo of preheater lime kiln. (Courtesy of Graymont, Inc., Cricket Mountain Plant.)

can range between a low of 25 m/s and a high of about 60 m/s. These are significantly lower than cement kilns, which operate around 80–100 m/s. The momentum ratio and associated Craya-Curtet parameter is usually lower than 2, which means the burner jet recirculation will have eddies and that fuel/air mixing is moderate and the flame is less intense than that in dead-burnt dolomite kilns or cement kilns. A simple heat and mass balance for the kiln section of a lime-making process is shown in Figure 10.5.

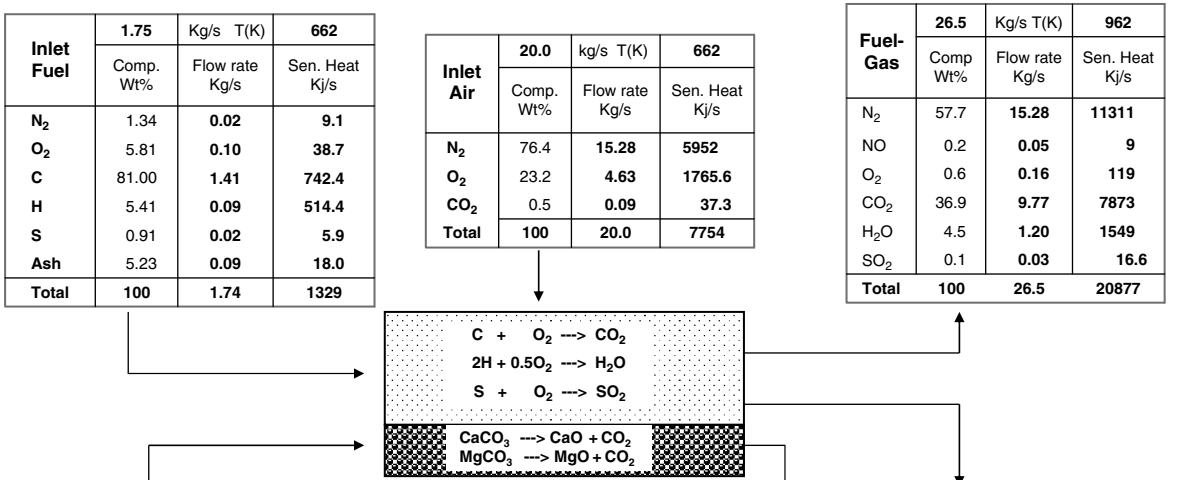

Inlet Fuel	1.75	Kg/s T(K)	662
	Comp. Wt%	Flow rate Kg/s	Sen. Heat Kj/s
N_2	1.34	0.02	9.1
O_2	5.81	0.10	38.7
C	81.00	1.41	742.4
H	5.41	0.09	514.4
S	0.91	0.02	5.9
Ash	5.23	0.09	18.0
Total	100	1.74	1329

Inlet Air	20.0	kg/s T(K)	662
	Comp. Wt%	Flow rate Kg/s	Sen. Heat Kj/s
N_2	76.4	15.28	5952
O_2	23.2	4.63	1765.6
CO_2	0.5	0.09	37.3
Total	100	20.0	7754

Fuel-Gas	26.5	Kg/s T(K)	962
	Comp Wt%	Flow rate Kg/s	Sen. Heat Kj/s
N_2	57.7	15.28	11311
NO	0.2	0.05	9
O_2	0.6	0.16	119
CO_2	36.9	9.77	7873
H_2O	4.5	1.20	1549
SO_2	0.1	0.03	16.6
Total	100	26.5	20877

Lime-stone	11.7	Kg/s T(K)	283
	Comp. Wt%	Flow rate Kg/s	Sen. Heat Kj/s
$CaCO_3$	95.3	11.11	–133.8
$MgCO_3$	0.0	0.00	0.0
H_2O	3.0	0.35	–10.2
S	0.0	0.00	0.0
Inerts	1.7	0.20	–1.3
Total	100	11.7	–145

Lime Prod.	6.00	kg/s T(K)	1200
	Comp. Wt%	Flow rate Kg/s	Sen. Heat Kj/s
$CaCO_3$	12.79	0.77	976.0
CaO	82.29	4.94	5225.6
$MgCO_3$	0.00	0.000	0.0
MgO	0.00	0.00	0.0
S	0.00	0.00	0
Inerts	4.92	0.30	175.3
Total	100	6.00	6377

Dust	0.9	Kg/s T(K)	962
	Comp. Wt%	Flow rate Kg/s	Sen. Heat Kj/s
$CaCO_3$	13.4	0.12	104.9
CaO	86.6	0.79	570.4
$MgCO_3$	0.0	0.00	0.0
MgO	0	0.00	0.0
S	0.00	0.00	0.0
Inerts	0.0	0.00	0.0
Total	100	0.92	675

Figure 10.5 Lime kiln heat and material balance.

10.4 The Cement Making Process

Rotary kilns are synonymous with cement making, the rotary kiln being the workhorse of that industry. There are all types of rotary kiln arrangements for producing cement clinker with each incremental design goal aimed at improving energy efficiency, ease of operation, and product quality, and minimizing environmental pollutants. Rotary cement kilns can be classified into wet-process kilns, semi-dry kilns, dry kilns, preheater kilns, and precalciner kilns. All of these are described in the book by Peray (1986) and many others, hence we will not dwell upon them here. Rather, we will briefly show the pertinent process chemistry and the heat requirements that drive them so as to be consistent with the transport phenomena theme.

10.5 The Cement Process Chemistry

The raw mixture of the cement kiln feedstock (or charge, raw meal) includes some formulations of limestone ($CaCO_3$), alumina (Al_2O_3), hematite (Fe_2O_3), and silica (SiO_3). As we discussed earlier, in its journey through the kiln, the charge undergoes all kinds of processes depending on the temperature, including drying, preheating, chemical reactions, a phase change, restructuring or sintering, and cooling. For kilns equipped with preheaters and precalciners (Figure 10.6) all the drying and some of the calcination reactions, for example, partial or full dissociation of limestone, take place there before entering the kiln proper. When the kiln feed enters the high temperature zones in the rotary kiln, a series of chemical reactions occur in which the quicklime, alumina, ferric oxide, silica, and other metal oxides react to form four main compounds of cement (Wang et al., 2006) namely, $CaO \cdot SiO_2$ (C_3S), $2CaO \cdot SiO_2$ (C_2S), $3CaO \cdot Al_2O_3$ (C_3A), and $4CaO \cdot Al_2O_3 \cdot Fe_2O_3$ (C_4AF). The formation temperatures of these compounds differ, which therefore defines the axial zones in which each compound is formed. The kiln's axial temperature profile can be divided by three zones where all the reactions occur either independently or simultaneously. These delineations include: (i) the decomposition zone (900°C), (ii) the transition zone (900–1300°C), and the sintering zone (1300–1400°C).

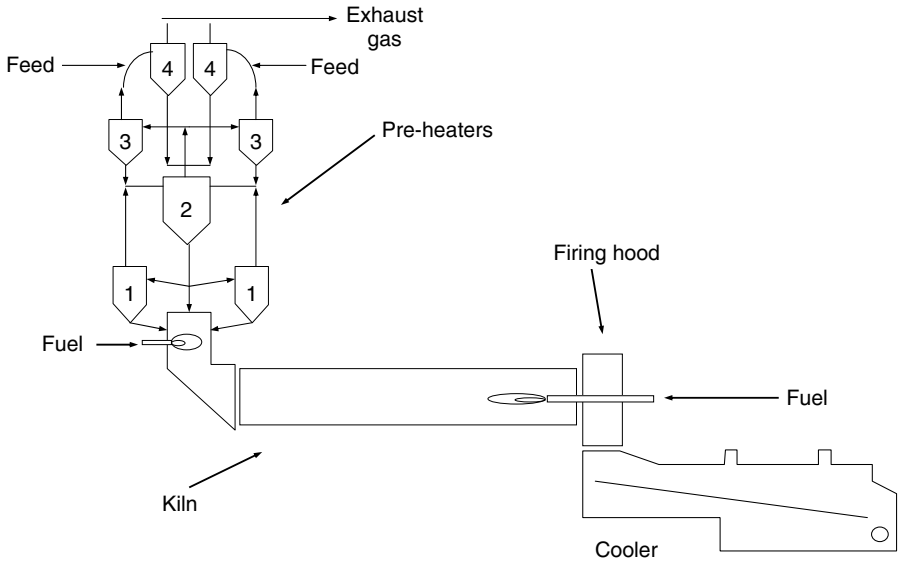

Figure 10.6 Typical schematic of a cement kiln with preheater, precalciner, and grate cooler.

10.5.1 Decomposition Zone

The amount of unreacted raw material in the outlet of the precalciner can be as much as 85–95 percent (Wang et al., 2006). Upon entering the decomposition zone small amounts of $CaO \cdot Al_2O_3$ (CA), $CaO \cdot Fe_2O_3$ (CF), $2CaO \cdot Fe_2O_3$, and $5CaO \cdot 3Al_2O_3$ (C_5A_3) are formed following the reactions below

$$CaCO_3 = CaO + CO_2 \quad (600\text{–}900^\circ C) \tag{10.10}$$

$$CaO + Al_2O_3 = CaO \cdot Al_2O_3 \quad (800^\circ C) \tag{10.11}$$

$$CaO + Fe_2O_3 = CaO \cdot Fe_2O_3 \quad (800^\circ C) \tag{10.12}$$

$$CaO + CaO \cdot Fe_2O_3 = 2CaO \cdot Fe_2O_3 \quad (800^\circ C) \tag{10.13}$$

$$3(CaO \cdot Al_2O_3) + 2CaO = 5CaO \cdot 3Al_2O_3 \quad (900\text{–}950^\circ C) \tag{10.14}$$

After the decomposition zone, that is, at the location with axial temperature greater than 900°C, it can be assumed that the dissociation of calcium carbonate, Equation (10.10), an endothermic reaction with $\Delta H = -1660\,\text{kJ/kg}\ CaCO_3$, is essentially complete.

10.5.2 Transition Zone

The key reactions in this zone are exothermic beginning with silica (C_2S), ($\Delta H = +603$ kJ/kg C_2S) followed by the formation of C_4AF($\Delta H = +109$ kJ/kg C_4AF), and C_3A($\Delta H = +37$ kJ/kg C_3A), that is,

$$2CaO + SiO_2 = 2CaO \cdot SiO_2 \quad (1000°C) \tag{10.15}$$

$$3(2CaO \cdot Fe_2O_3) + 5CaO \cdot 3Al_2O_3 + CaO = 3(4CaO \cdot Al_2O_3 \cdot Fe_2O_3) \quad (1200–1300°C) \tag{10.16}$$

$$5CaO \cdot 3Al_2O_3 + 4CaO = 3(3CaO \cdot Al_2O_3) \quad (1200–1300°C) \tag{10.17}$$

10.5.3 Sintering Zone

In this zone liquidus phase reactions are formed. The main component, C_3S ($\Delta H = +448$ kJ/kg C_3S), is formed by a reaction between C_2S formed earlier and any available free lime as,

$$2CaO \cdot SiO_2 + CaO = 3CaO \cdot SiO_2 \quad (1350–1450°C) \tag{10.18}$$

The kinetic rate constants for the dissociation, Equation (10.10), and Equations (10.15) through (10.18) assembled by Guruz and Bac (1981) are presented in Table 10.2. Similar rates were obtained by Mastorakos et al. (1999) by trial and error to give the expected (measured) composition of charge at the exit of cement kilns.

Obviously these equations are by no means the only reactions involved, since there are traces of other metal oxides that evolve or

Table 10.2 Parameters for Reaction Rate Constant, $k = A \exp(-E/RT)$.*

Reaction	Frequency Factor, A (1/hr)	Activation Energy (kJ/kg mol)
$CaCO_3 = CaO + CO_2$	9.67×10^{24}	1,092,947
$2CaO + SiO_2 = C_2S(2CaO \cdot SiO_2)$	1.41×10^{15}	346,014
$CaO + C_2S = C_3S(3CaO \cdot SiO_2)$	4.18×10^{8}	461,352
$3CaO + Al_2O_3 = C_3A(CaO \cdot Al_2O_3)$	1.81×10^{9}	251,208
$4CaO + Al_2O_3 + Fe_2O_3 = C_4AF(4CaO \cdot Al_2O_3 \cdot Fe_2O_3)$	5.59×10^{11}	188,406

* Note that the following combinations are given in shortened form: $2CaO \cdot SiO_2$ (C_2S), $CaO \cdot SiO_2$ (C_3S), $3CaO \cdot Al_2O_3$ (C_3A), and $4CaO \cdot Al_2O_3 \cdot Fe_2O_3$ (C_4AF).

go into reaction as well. For example, magnesia, MgO, from the dissociation of $MgCO_3$, which usually accompanies $CaCO_3$ as dolomite or dolomitic magnesia, will, as we saw under lime kilns, undergo reactions similar to quicklime. It is said that the maximum permissible MgO in clinker should not exceed 6 percent. Alkaline metals such as potassium and sodium and also sulfur are present in the cement feedstock. K_2O generally enters the raw meal as a natural mineral in the form of $K \cdot AlSi_3O_6$ and exits with the clinker as K_2SO_4. It is often referred to as double alkali salt, since Na_2SO_4 also forms similarly, or in an even more complex form (Haspel, 1998). Sulfur also enters the kiln system through the raw material or fossil fuels used for combustion and forms in the clinker as SO_3. The sulfur that is exhausted from the kiln through the exhaust gas stream does so as SO_2. Various sulfur and alkali cycles exist in the rotary cement kiln and, when proper measures are not taken to have them bypass the heat transfer surfaces, they can condense on the heat transfer surfaces, causing them to foul. Obviously, there is more to cement making than described here, and readers interested in a more detailed process description, including the effect of each component on cement quality, should refer to the appropriate text.

10.6 Rotary Cement Kiln Energy Usage

The distribution of energy within the cement-making process is based on the theoretical minimum process heat of formation of the clinker (Table 10.3) (Haspel, 1998). From the table, the theoretical minimum process heat required to form 1 kg of clinker, which is defined as the difference between heat input and heat output of the process, is about 420 kcal/kg (about 1.5 MBtu/ton). This amount will decrease if the process is carried out in a rotary kiln equipped with preheater. Although this energy accounts for heat losses through the ancillary equipment (Table 10.4) the bulk of it (about 52 percent) goes to the transformation of the raw meal into clinker material. The energy usage or the specific heat consumption is about 800 kcal/kg clinker (2.88 MBtu/ton) compared to about 6 MBtu/ton for a lime-making kiln with preheater. This is because of the exothermic reactions associated with the clinker-making process and perhaps more efficient preheating systems, given the fact that the raw material is fed as powder with high particle surface area, thereby enhancing gas-solid heat exchange in the cyclone preheaters.

Table 10.3 Theoretical Minimum Process Heat of Formation of Cement Clinker

Event/Process	Temperature Range (°C)	Energy (kcal/kg clinker)
Heat in		
Sensible heat to raw material at temperature	20–450	170
Dehydration of clay at temperature	450	40
Sensible heat into raw material at	450–900	195
Dissociation of $CaCO_3$ at	900	475
Sensible heat into material at	900–1400	125
Net heat of melting	1400	25
Subtotal	20–1400	1030
Heat out		
Exothermic crystallization of dehydrated clay	—	10
Exothermic formation of cement compounds	—	100
Cooling of clinker	1400–1420	360
Cooling of CO_2	900–920	120
Cooling and condensing of steam	450–470	20
Subtotal	1400–1420	610
Theoretical minimum process heat required to form 1 kg of clinker		420

Table 10.4 Typical Cement Kiln Heat Balance (Haspel, 1998)

Heat Loss/Transfer	Kcal/kg Clinker	Percent of Total (800 kcal/kg basis)
Raw meal to clinker	417	52.1
Preheater exhaust	183	22.9
Cooler exhaust	78	9.8
Clinker discharge	17	2.1
Dust loss	17	2.1
Shell loss	88	14.75
Total	800	100

Cement kilns have been successfully modeled using the chemistry described above with the one-dimensional zone method for radiation heat transfer (Guruz and Bac, 1981) with plausible results. They have also been recently combined in commercial CFD packages for example that offered by CINAR. Mastorakos et al. (1999) modeled the chemistry

with an axisymmetric commercial CFD code (FLOW-3D) and obtained axial concentration of species similar to the one-dimensional concentration profiles reported by Guruz and Bac (1981).

10.7 Mineral Ore Reduction Processes in Rotary Kilns

In the field of extractive metallurgy, solid state reduction of oxide ore is an important beneficiation process. Reduction of oxide minerals in the presence of suitable reducing compounds or elements (reductants) to metallic state or to lower oxide levels enables changes in the grain structure and the chemical activation in downstream pyrometallurgical metal extraction processes such as an electric arc furnace. The reductants for the direct reduction of iron ore used in the production of sponge iron and some important oxides such as rutile (TiO_2) can be either in a gaseous state (CO and H_2) or in the solid state (carbon). The latter route, known as carbothermic reduction process employs the rotary kiln as the primary roasting (calcination) reactor. We will examine two carbothermic reduction processes the SL/RN process for DRI and the Becher process for the carbothermic reduction of ilmenite ore, which employ rotary kilns as their primary reactor.

10.7.1 The Rotary Kiln SL/RN Process

SL/RN is an acronym for steelmaking companies Stelco, Lurgi, and Republic National. The process essentially involves a rotary kiln in which both solid reductant and the oxide ore are fed at one end and direct reduction iron (DRI) is collected at the opposite end. The ability of this process to use a wide range of carbonaceous matter comes from an important advantage the rotary kiln offers. The kiln allows the coexistence of a reducing bed and an oxidizing freeboard at the same axial location, something unique to rotary kilns. The first DRI plant based on the SL/RN process was established in the 1960s by Lurgi Metallurgie, the predecessor of Outotec Oyj. Since then there have been a number of commercial plants commissioned worldwide operating with the widest range of iron bearing materials including pellets, lump ores, beach sand, and ilmenite ore. The wide range of reductants used includes anthracite, bituminous and sub-bituminous coals, lignite, petroleum coke, and charcoal from biomass.

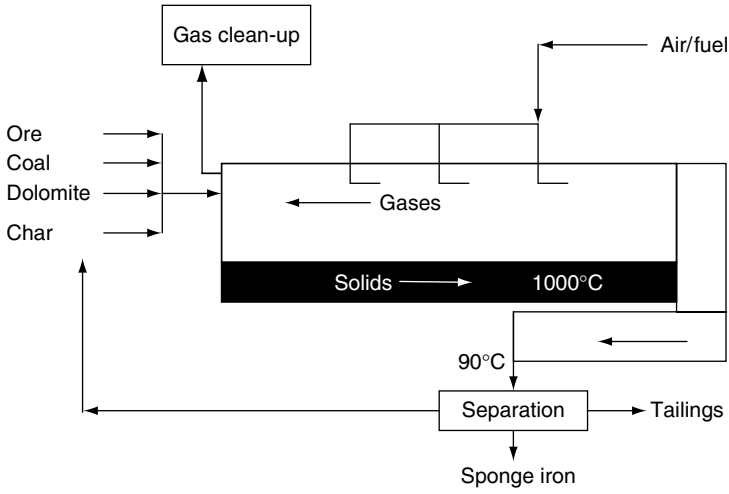

Figure 10.7 Schematic of the SL/RN process.

The kiln process can be described as per the schematic of the layout shown in Figure 10.7 (Venkateswaran and Brimacombe, 1977). The rotary kiln is charged with iron ore along with coal, recycled char, and dolomite. Some SR/LN kilns operate on a mixture of iron sand and char in a 10:3 ratio. The purpose of adding dolomite is to scrub the sulfur in the coal, if needed. Air is blown into a countercurrent freeboard with onboard (shell) fans located at several positions along the kiln's axial length. Because the bed is under reducing conditions, the onboard fans sustain combustion of evolved gas into the freeboard. Although the coal in the charge provides the energy needed to drive the process, provision is made for the supply of auxiliary fuel. Unlike cement, where four reaction zones can be distinguished, in the SR/LN process there are two major zones of interest, that is, a preheat zone (about 40–50 percent of axial length) and a reduction zone. The span of the preheating zone is large, encompassing all the rotary kiln sequential process beginning from drying, coal devolatilization, and the dissociation of dolomite, if present. Also in the preheat zone, the hydrogen released during the devolatilization of coal initiates DRI, that is, "prereduction" of the iron ore. As the charge advances axially and reaches a temperature in excess of 900°C, the reduction zone begins where the reduction reactions ensue. There is a two-step process that begins with the Boudouard reaction whereby the carbon in the char, a product of the coal devolatilization reaction in the preheat zone, reacts with CO_2

to yield CO. The CO, in turn, reacts with the iron sand or iron oxide pellet or metallic iron in the following reactions

$$C + CO_2 = 2CO \tag{10.19}$$

$$Fe_xO_y + CO = Fe_xO_{y-1} + CO_2 \tag{10.20}$$

The overall reaction for Fe_2O_3 and FeO are

$$Fe_2O_3 + 3C = 2Fe + 3CO \tag{10.21a}$$

$$FeO + C = Fe + CO \tag{10.21b}$$

Because the Boudouard reaction is highly endothermic, char reactivity is an essential process consideration. Owing to the lack of external preheaters and precalciners as encountered in cement processing, the retention time for an SR/LN kiln with a 4.1 m diameter and 65 m length processing about 40 metric tons/hr iron sand and rotating at 0.5 rpm is in the 8–12 hr range. As in all heterogeneous reactions, good granular mixing is essential to achieving an efficient operation. Mixing is even more important in carbothermic processes because the reactions involve several solid-gas interactions, which might be subject to mass transfer limitations associated with packed beds and slow rotational rates. With the density differences between the sand and char/coal, the process can also encounter severe axial and radial segregation patterns, which can manifest themselves into temperature and concentration gradients. These shortcomings can lead to product quality issues if mixing is inadequate. Venkateswaran and Brimacombe (1977) modeled the SR/LN process using the bed chemistry and the zone-type radiative heat transfer model described in Chapter 7 with considerable success. Such models have been extended to other carbothermic reduction processes such as ilmenite and laterite ore reduction in rotary kilns (Nicholson, 1995).

10.7.2 Roasting of Titaniferous Materials

The success of the carbonaceous reduction of iron oxide has opened doors for the beneficiation of other minerals that coexist with oxides of iron also known as mineral sands. Examples of these ores are ilmenite, containing titanium dioxide and laterite ore, containing nickel oxide. Titanium dioxide (TiO_2) is one of the most important inorganic materials used as a pigment for paper, plastics, paints, textile, and so on.

Titanium metal is also used to produce various types of surgical equipment, and used extensively in the aerospace industry. Rutile, an almost pure TiO_2, is the preferred mineral precursor for titanium extraction. However, with its limited availability and recent instabilities encountered in rutile-rich deposit regions, efforts have intensified to exploit the more abundant titaniferous ilmenite ($Fe_2O_3 \cdot TiO_2$). In order to render it as a suitable feedstock, it is necessary to upgrade these mineral ores by selective removal of the iron and thereby enrich the TiO_2 to a grade known in the industry as synthetic rutile. Selective removal of iron from ilmenite minerals has been an area of extensive growth and a number of beneficiation processes have been suggested and tried. The most commonly practiced process of considerable importance is the thermal treatment (roasting) of titaniferous materials, for example, ilmenite ore in a rotary kiln, known as the Becher process (Becher, 1963). The Becher process involves several steps beginning with a reduction, in rotary kiln, of the iron oxides contained in the ilmenite feedstock largely to metallic iron using coal as the reductant as is done in the DRI process (Figure 10.8). This results in a mixture of metallic iron and titanium phases known as "reduced ilmenite." It has been reported (Welham, 1997) that the solid state pre-reduction of ilmenite by carbon takes place at $>400°C$, followed by a carbon monoxide reduction to elemental iron at $>1000°C$. After cooling and discharging from the reduction kiln the product is dry-separated to remove the reduced iron and the excess char remaining after the reaction. The reduced ilmenite is then subjected to aqueous oxidation (also know as aeration) to convert the metallic iron to iron oxide particles discrete from the TiO_2-rich mineral particles. Aeration is followed by a wet physical separation to remove the iron oxide enriching the mix to synthetic rutile. Depending on the desired purity, further refinement might be carried out to remove the residual iron and traces of manganese and magnesium that naturally coexist with the ore using acid leaching followed by washing, dewatering, and drying.

The first commercial plant that employed the Becher process was built by Lurgi Metallurgie, the predecessor of Outotec, Oyj in 1968 following the SR/LN experience. It was for the reduction of Australian ilmenite at Western Titanium N.L. at Capel, Australia. It consisted of a 2.4 m diameter by 30 m long rotary kiln and is still in operation. It opened up many possibilities for the beneficiation of ilmenite to synthetic rutile without the consumption of acids and the generation of acidic iron effluents as associated with hydrometallurgical processes. Lurgi later built a slightly larger rotary kiln in 1969 (4 m diameter by

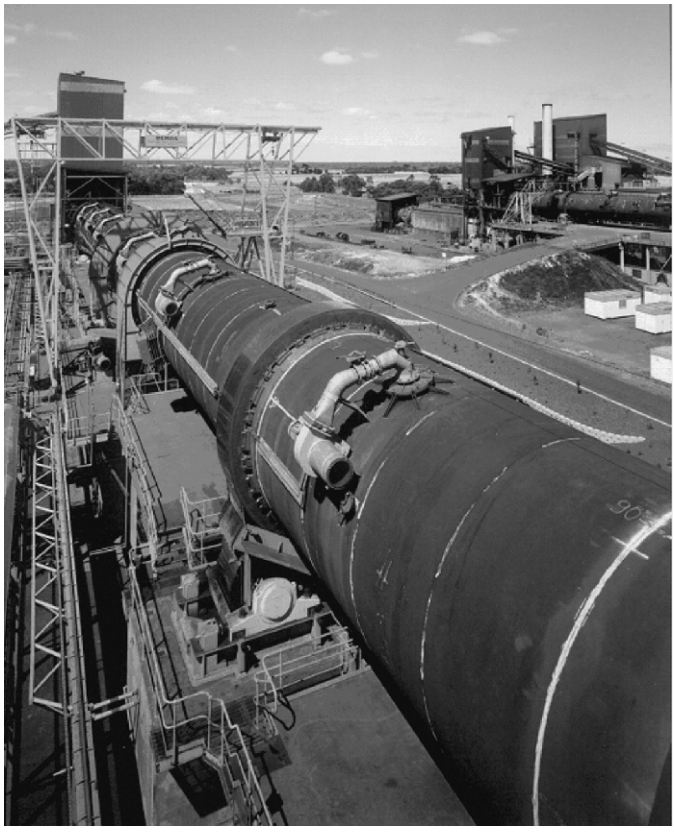

Figure 10.8 The Becher process kiln with onboard fans. (Courtesy of Outotec Oyi.)

75 m long kiln) at New Zealand Steel Corporation at Glenbrook for processing TiO_2 containing iron sands ($FeTiO_3$). Instead of a long kiln, a moving grate preheater can be installed upstream of the rotary kiln where prehardened green pellets containing iron sands and lignite reductant can be heated to a prereduction temperature using waste gases from the rotary kiln. The Becher process has undergone a tremendous improvement thanks to research at CSIRO, which embarked on several mechanistic modeling and engineering endeavors aimed at understanding the chemistry and operation of the process (Nicholson, 1995). Figure 10.9 shows the 4.6 by 68 m rotary kiln for direct reduction of ilmenite concentrates with subbituminous coal at Iluka Resources I, Australia built in 1984. It has a capacity of 900,000 metric tons per year ilmenite feed.

Figure 10.9 4.6 by 68 m rotary kiln for direct reduction of ilmenite concentrates with subbituminous coal at Iluka Resources I, Australia built in 1984. Capacity: 900,000 metric tons per year ilmenite feed. (Courtesy of Outotec, Australasia, Pty).

10.8 The Rotary Kiln Lightweight Aggregate Making Process

A process that does not involve a purely chemical reaction but a combination of both physical and chemical ones is the processing of shale, clay, or slate at high temperatures (900–1200°C) in a rotary kiln to produce a lightweight aggregate. Lightweight aggregate belongs to the general body of aggregates used for mortar, plaster, concrete, and other masonry works. Naturally occurring lightweight aggregates are pumice, lava, slag, burned shale, slate, and clay. These lightweight aggregates are similar to other naturally occurring aggregates such as stone and sand in particle shape and gradation except for the aggregates' weight (some aggregates float on water). The aggregates'

lightness is attributable to the multitude of tiny pores generated within each particle during formation. The origin of the lightweight aggregate industry as it is known today can be traced to shipbuilding in the early 1900s. Studies at the time by marine engineers indicated that a concrete ship would be practical if the concrete used could meet strengths exceeding 35 MPa (5 psi) at a density less than 1760 kg/m^3 (110 lb/ft^3). Extensive investigations revealed that while naturally occurring lightweight aggregates could not meet these specifications, rotary-kiln-produced expanded shale could. The American shipbuilding authority then commissioned one Stephen J. Hayde to develop a strong, inert, and durable lightweight aggregate from shale, slate, and clays in the rotary kiln. Shipbuilding during the great wars took advantage of this development and made extensive use of rotary kiln produced lightweight aggregate for constructing ship decks. Since then the lightweight aggregate industry has employed the rotary kiln as the primary device for high temperature processing of shale, slate, or clay achieving densities lower than 440 kg/m^3. For further reading on this role, the reader is referred to Holm (1995).

The thermal treatment of shale, slates, and clay to produce lightweight aggregate involves the expansion of the material as a result of an evolution of gases at elevated temperatures. Upon heating, the shale, slate, or clay particle undergoes a sequential process beginning with drying, followed by preheating, then expansion (also known as bloating). The last step occurs as particle temperature approaches the 900–1000°C (1650–1830°F) range, and is believed to be caused by bloating agents such as CO_2 that evolve as the compounds in the raw material decompose. Because there is no appreciable mass loss associated with the bloating process, an increase in volume results in a decrease in specific gravity, a property that is important to structural concrete applications of lightweight aggregate. In addition, the porous structure that results from bloating gives lightweight aggregates the added advantage of enhanced thermal and acoustical insulating properties (Holm and Bremner, 1990). Today, applications are found in many masonry works such as high-rise building construction, roofing, bridge decks, and so on. In the 1950s, it was used to roof the House and Senate wings of the U.S. Capitol (Figure 10.10) and to deck the Chesapeake Bay Bridge in Maryland. Mechanical properties, strength and notable engineering applications of rotary kiln lightweight aggregates and concrete are widely published in the open literature (Holm, 1995; Holm and Bremner, 1990).

Figure 10.10 Concrete replacement with LWA structural concrete on the roof of the U.S. Capitol by Southern Lightweight Aggregate Corporation, later Solite Corporation of Richmond, sometime in 1950s. (Courtesy of Northeast Solite Corporation.)

In the United States today there are many lightweight aggregate (LWA) manufacturing companies some of which have been in operation for over 60 years. Many of these can be easily identified by the suffix "lite," which appears to be associated with the lightness of the material. The nature of the rotary kiln, which allows flame residence times on the order of 2–5 s and temperatures of over 2000 K (3100 F), also gives such kilns a competitive alternative to commercial incinerators of organic wastes and solvents. Today, there are a handful of LWA manufacturing facilities that use such wastes as supplemental fuels for combustion. Such kilns are regulated by the United States Environmental Protection Agency (EPA) as industrial furnaces

and operate under the Boiler & Industrial Furnace (BIF) compliance act. Like all rotary kiln processes, achieving product uniformity is the key attribute to achieving the early shipbuilder's dream of light, strong, and durable material. This, coupled with the responsibility of protecting the environment, makes LWA manufacturing a challenging task.

10.8.1 LWA Raw Material Characterization

We mentioned that bloating or the expansion of slate, shale, or clay occurs at high temperatures in rotary kilns. In essence, the temperature window at which expansion occurs is quarry dependent. Even within the same quarry this temperature window may change from strata to strata (or from bench to bench). In order to maintain a certain product quality it is important to keep track of the mining operation to provide assays of the deposits so as to adjust the kiln temperature profiles to match their expansion rate. Figure 10.11 shows the mining of shale deposits strata by strata.

Figure 10.11 Mining of shale feedstock for high-temperature rotary kiln lightweight aggregate. (Courtesy of Utelite Corporation, Coalville, UT.)

10.8.2 LWA Feedstock Mineralogy

The mineralogy of shale, slates, and clays that bloat when subjected to elevated temperatures has been widely reported (Boateng, et al., 1997; Epting 1974). These minerals generally constitute, by volume, 80–97 percent mica clay, 0–10 percent quartz-feldspar, and 2–7 percent accessory minerals, for example, calcite, pyrite, and so on. X-ray analyses have indicated that the major mica-clay constituent of expandable materials is either kaolinite or montmorillonite in still clays, illite and chlorite in the slightly metamorphosed mudstones (shale), and muscovite and chlorite in the more strongly metamorphosed slates. Assays on the raw materials indicate that the oxides may be grouped as shown in Table 10.5.

There has been a considerable amount of discrepancy on the origin of the gas producing agent that causes bloating. Ehlers' work (Ehlers, 1958) suggested that the bloating agents are calcite, $CaCO_3$, and ankerite, $Ca(Fe, Mg)(CO_3)$, both of which decompose at around 923°C (1693°F), and that the gases that cause bloating are CO_2 and traces of SO_2. Later, Phillips (1974) surveyed all the relevant literature and concluded that most of the mica-clay deposits can absorb various types of hydrocarbons and reasoned that as a result, they can retain some of their hydroxyl water beyond its major loss at the 500–700°C (932–1292°F) range, suggesting dehydroxylation as the cause of bloating. Notwithstanding, he concluded that CO_2 is the single gas common to the bloating of all the expandable materials. Differential thermal analysis (DTA) work (Epting, 1974) on these minerals indicate that there is an endothermic loss of bound water (dehydroxylation) at 600°C (1112°F) and another endothermic reaction at a relatively higher temperature around the 900–1200°C (1652–2192°F) range. The latter reaction may perhaps substantiate the claim that CO_2

Table 10.5 Metal Oxide Composition of Expanded Shale, Clay, and Slate (Boateng et al., 1997)

Compound	Percent
SiO_2	61–73
Al_2O_3	11–26
Fe_2O_3	3.5–9
Oxides of Ca, Mg, Na, and K	<5
Loss on ignition	≈ 0.12

is the bloating gas and that it evolves by the decomposition of calcite as claimed by Ehlers or, perhaps, by subsequent reduction reactions involving carbon.

Work on kinetics of the bloating of shale, slate, or clay has been lacking. However, there is little doubt that the process involves heterogeneous gas-solid chemical reactions coupled with a mass transfer phenomenon. Such reactions may proceed through the following three steps (Boateng et al., 1997) as: (i) chemical reaction involving the evolution of gas; (ii) diffusion of the gaseous product through the core of the particle; and (iii) diffusion of the gas through the outer boundary of the particle. Although it is not readily known which one of the three steps controls particle expansion, the internal voids created by the process suggest that the gases evolve at a rate faster than they can diffuse through the particle. Furthermore, like most ceramic materials, thermal conductivity tends to decrease at elevated temperatures (Zdaniewski et al., 1979) so that fusion of the periphery of the particle may lead to the formation of a pyroplastic exterior that is likely to increase the resistance to gas transport to the outer boundary layer. This phenomenon results in swelling with almost negligible mass loss. Since the particle is sealed on the periphery, the work done by internal gas movement goes to generate the internal porous structure. The low specific gravity of an LWA product is a result of volume increase with negligible mass loss.

To determine the extent of bloating or expansion in an industrial rotary kiln, one must carry out laboratory tests using bench scale furnaces for the evolution kinetics and further correlation tests in a pilot rotary kiln for appropriate temperature profiles. The temporal events determined are, in turn, used to plan quarry operations for product quality control. The same data may also be useful in developing a mechanistic mathematical model that can predict temperature distribution and density changes in the raw material as they journey through the kiln (Boateng et al., 1997). Such tools have proven to be useful for the control of product quality as new mines are explored or even as different strata of the existing mine are explored for feedstock. Some of these time-temperature histories are discussed herein.

10.8.3 LWA Thermal History

The physical events that occur as a shale, clay, or slate particle undergoes temperature changes can first be explored in the laboratory by

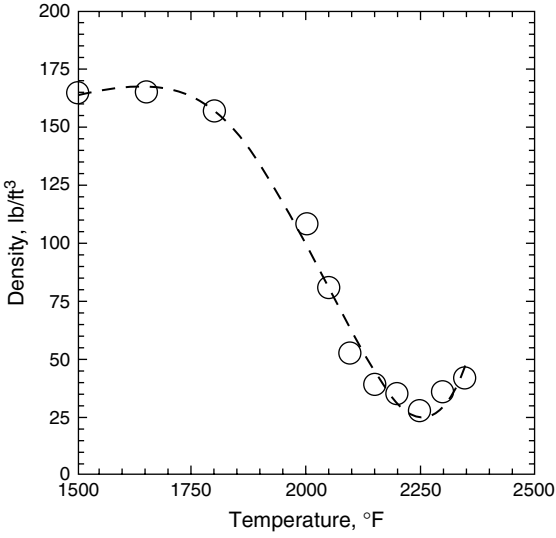

Figure 10.12 Density versus temperature curve for expanded shale precursor.

various techniques. Thermogravimetric analysis, TGA used for coal characterization, is usually employed to determine the temperature at which mass changes occur in a sample. For instance, the temperature at which evaporation of free moisture or volatile evolution occurs can be established using this technique. Since there is no appreciable mass change during bloating itself, TGA is not appropriate for characterizing shale, slate, or clay expansion in the LWA making process. TGA data on materials from a Virginia mine (Figure 10.12) shows that there is a progressive decrease in sample density within the 1950–2150°F (1066–1778°C) temperature range but within the same range the percent weight loss remains unchanged. Differential thermogravimetric analysis (DTA), on the other hand, can be used to establish the temperature ranges where any chemical reaction is likely to occur.

The density changes as a function of temperature and time can be established by following standard ASTM methods for measuring density. Usually the particle is placed in a muffle furnace that is set at a predetermined temperature and is removed at a predetermined time. This is followed by a density test. Successive repetition of the procedure will map out density-temperature history. Since some expanded shale, clay, or slate may float on water, at times some of these experiments are carried out using kerosene as the displacement agent. As seen from

Figure 10.12, the density drop for this particular material begins at 1600°F (870°C) and achieves the lowest density at 2250°F (1232°C) after which density rebound occurs as a result of pore collapse (vitrification). The expansion or coefficient of expansion, for that matter, can be determined using dilatometry. This is a technique employed to measure the change in length of a specimen as a function of temperature. The slope of the change in length per unit starting length is the coefficient of linear expansion. Highly metamorphosed shale (or slate) from quarries in the North Carolina area and the Hudson Valley in New York require a slightly higher temperature than the others to achieve complete expansion. From these it is possible to determine the activation energies for the expansion process from which kinetic models can be developed for each quarry and used for quality control of the LWA. Density-temperature plots for several expanded shale and clay precursors from some quarries in the Eastern Seaboard of the United States and their likely kinetic data are shown in Figure 10.13 (Boateng et al., 1997). The activation energy for the expansion or bloating lies in the 30–70 kJ/mol range.

The tests described in the preceding section are carried out in a muffle furnace and are only useful as a first step in quantifying the behavior of the raw material. Specifically, they are only good for fundamental work on prospecting new quarries. For the purpose of designing large

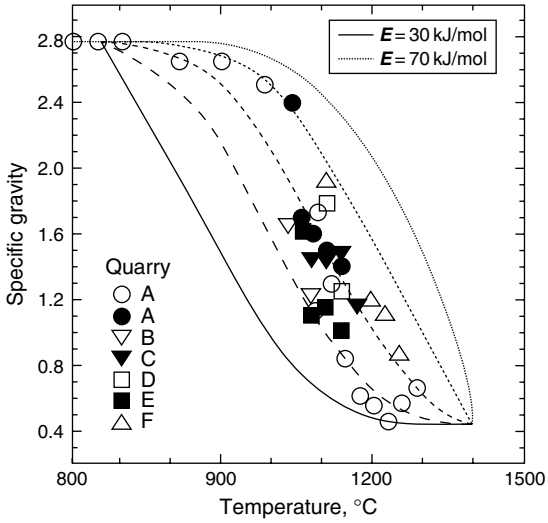

Figure 10.13 Density-temperature curves for expanded shale or clay raw materials from several quarries. Note: *E* lies between 30–70 kJ/mol.

rotary kiln operations or in order to properly simulate the rock behavior in an industrial rotary kiln, pilot kiln studies are essential. It is a good engineering practice to collect yearly pilot kiln data on all samples so as to establish where to mine, what material requires extra heat and which one gives better weights, etc.

Figure 10.14 shows typical pilot kiln test results for intermediate strata material from two quarries. The plot also shows the effect of raw material gradation on product density. Most LWA correlation tests have shown that product quality improves with quarry depth. This is in part due to the fact that the rock from the top bench is likely to be withered by atmospheric conditions. As Figure 10.14 shows, there is a significant difference between the product qualities with regard to feeding coarse particles as compared to feeding fine particles. These tests reinforce that interparticle voids play a key role in bed heat transfer. More importantly the variation in particle size impacts greatly on quality as smaller particles in a mix of larger ones will tend to segregate to the core and will not receive adequate heat. Depending on the raw material type and the operating conditions in the kiln, unit weights of the clinker can range between 45–65 lb/ft^3 for most LWA. Data also show that at a temperature of 2100°F, the same material will expand to 28 lb/ft^3 if it is retained for an additional 5 minutes. This means

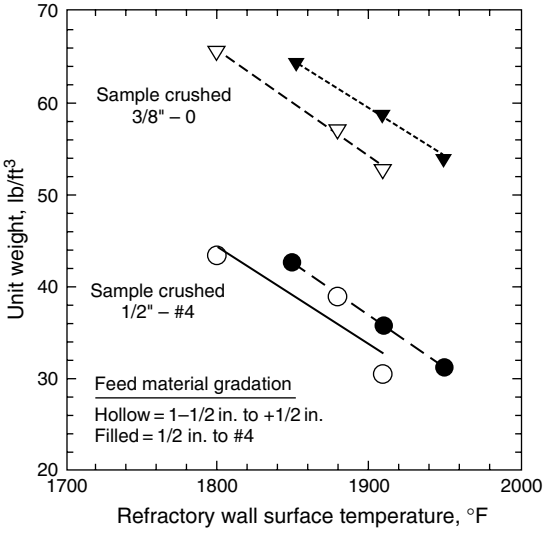

Figure 10.14 Unit LWA weight (density) as a function of rotary kiln temperature.

Figure 10.15 Combustion zone region of an LWA kiln with material at incipient fusion. (Courtesy of Utelite Corporation, Coalville, UT.)

that careful control of the kiln's temperature profile is essential due to the narrow temperature window within which one needs to operate to achieve the desired quality. Owing to the narrow temperature window of expansion for most of these materials, LWA kilns are prone to severe agglomeration, forming large balls at the burning zone that have the tendency of obstructing the operation. Figure 10.15 shows an incipient fusion of expanded shale in the combustion zone of an industrial LWA kiln. A trained eye will notice that the product is well expanded and ready for discharge. However, further increases in temperature can increase the size and can cause severe agglomeration if not discharged.

References

R. G. Becher. *Roasting of titaniferous materials*, Australian Patent # 247110, 1963.

A. A. Boateng, E. R. Thoen, and F. L. Orthlieb. "Modeling the pyroprocess kinetics of shale expansion in a rotary kiln," *Trans. IChemE*, 75, part A1, 278–283, 1997.

R. S. Boynton. *Chemistry and Technology of Lime and Limestone*. John Wiley & Sons, New York, 1980.

E. G. Ehlers. "Mechanism of lightweight formation," *Ceramic Bulletin*, 37(2), 95–99, 1958.

C. R. Epting. *Mechanism of Vesiculation in Clays*. MS Thesis, Clemson University, 1974.
H. K. Guruz and N. Bac. "Mathematical modelling of rotary cement kilns by the zone method," *Can. J. Chem. Eng.*, 59, 540–548, 1981.
D. W. Haspel. *Cement Handbook*. Summary of Key Data, Prolink Ltd. 1998.
T. A. Holm. Lightweight Concrete and Aggregates. In Standard Technical Publication STP, 169C, American Society for Testing Materials (ASTM), 1995.
T. A. Holm and T. W. Bremner. "70 Year Performance Record for High Strength Structural Concrete," Proceedings, First Materials Engineering Congress, August (American Society of Civil Engineers), Denver, CO, 1990.
E. Mastorakos, A. Massias, C. Tsakiroglou, D. A. Goussis, V. N. Burganos, and A. C. Payatakes. "CFD predictions for cement kilns including flame modelling, heat transfer and clinker chemistry," *Applied Mathematical Modeling*, 23(1), 55–76, 1999.
T. Nicholson. "Mathematical Modeling of the Ilmenite Reduction Process in Rotary Kilns," PhD Thesis, University of Queensland, 1995.
J. A. H. Oates. *Lime and Limestone, Chemistry and Technology, Production and Uses*. Wiley-VCH, Weinheim, 1998.
K. E. Peray. *The Rotary Cement Kiln*. Chemical Publishing Co., Inc., New York, 1986.
E. L. Phillips. Gas Producing Agents in Expansion of Shales, Slates, and Clays (Unpublished), 1974.
N. J. Themelis. *Transport and Chemical Rate Phenomena*. Taylor & Francis, New York, 1995.
V. Venkateswaran and J. K. Brimacombe. "Mathematical model of SR/LN direct reduction process," *Met. Trans. B.*, 8, 387–398, 1977.
S. Wang, J. Lu, W. Li, J. Li, and Z. Hu. "Modeling of pulverized coal combustion in cement rotary kiln," *Energy & Fuels*, 20, 2350–2356, 2006.
N. J. Welham. "A parametric study of the mechanically activated carbothermic reduction of ilmenite," *Materials Engineering*, 9(12), 1189–2000, 1996.
W. Zdaniewski, D. P. H. Hasselman, H. Knoch, and J. Heinrich. "Effect of oxidation on the thermal diffusivity of reaction-sintered silicon nitride," *Ceramic Bulletin*, 58(5), 539–540, 1979.